JOURNAL OF Materials CHEMISTRY

Vibrational spectra and thin solid films of a bi(propylperylenediimide)

S. Rodriguez-Llorente,[a] R. Aroca*[a] and J. Duff[b]

[a] *Materials and Surface Science Group. University of Windsor, Windsor, ON, Canada N9B 3P4*
[b] *Xerox Research Centre of Canada. 2660 Speakman Drive, Mississauga, ON, Canada L5K 2L1*

Received 24th April 1998, Accepted 19th July 1998

The synthesis, the fabrication of thin solid films and the optical spectra of a member of a new series of bis-perylene materials—the bi(propylperylenediimide), *N′,N‴*-dipropyl-*N,N″*-bi[perylene-3,4:9,10-bis(dicarboximide)] (Pr_2)—are reported. The objective of the present research effort is to provide the fundamental spectroscopic characterization of the ground electronic state and the methods for the fabrication of submicron thin solid films of these new materials which are being tested for performing elementary electrical functions of electronic devices. Pr_2 is a high molecular weight perylene dye and the molecular organization formed in vacuum evaporated nanometric films is one of the key elements determining the electrical and optical properties of thin solid films. The spectroscopic techniques used in the study of fundamental vibrational modes were transmission and reflection–absorption infrared spectroscopy (RAIRS). The inelastic scattering was investigated using out-of-resonance excitation (FT-Raman), resonance Raman scattering (RRS) and surface-enhanced resonance Raman scattering (SERRS) on silver island films. The vibrational assignment of characteristic wavenumbers was assisted with semi-empirical quantum mechanical calculations.

Introduction

The tendency to self-alignment observed in vacuum evaporated thin solid films of large aromatic molecules such as phthalocyanines and perylene tetracarboxylic (PTC) derivatives has been known for several decades,[1–3] however our understanding of the mechanism of film formation and growth is still far from complete. It is agreed that molecular thin solid films are assemblies of organic molecules bound by weak van der Waals forces. In aromatic molecules, flatness of the molecular plane and an extensive π system appear to be sufficient conditions for self-ordering.[4] It is found that molecular solids may exhibit various crystals forms that arise from different molecular stacking arrangements.[5] It is also known that the optical and electrical properties of organic materials are highly dependent on these crystal forms. Currently, ultrathin films of these materials are being intensively investigated to study the optimization of their optical and electronic properties for potential use in a variety of technological applications. In fact, high quality ultrathin films of perylene derivatives have been prepared using the Organic Molecular Beam Deposition (OMBD) technique which produces thin films with a good crystalline structure in ultra high vacuum. The objective of this work has been to obtain well-ordered organic films on inorganic single-crystalline substrate (epitaxial growth) and to investigate the relation between substrate orientation and film structure. Of the various PTC materials, most of the OMBD work has been focused on the growth of 3,4,9,10-perylenetetracarboxylic dianhydride (PTCDA).[6–10] Recently, Armstrong *et al.*[11] have grown ultrathin films of PTCDA and *N,N′*-di-*n*-butylperylene-3,4:9,10-bis(dicarboximide) on (001) alkali halide surfaces. A theoretical study of a perylene derivative on gold (111) has also been reported.[12] Our research effort is to investigate the electronic spectra, vibrational spectra and thin solid films of a new classes of PTC materials. We have previously reported the film fabrication and spectral properties of 1,3-bis(3-chlorobenzylimidoperylenyl)propane (BPTDPr), a molecule where the two PTC groups are attached to the ends of a propane molecule.[13] The work was complemented with the study of the effect of the chain length (propane *versus* octane) of the bisperylene in the molecular organization and aggregation in the solid films: the characterization of 1,8-bis(3-chlorobenzylimidoperylenyl)octane (BPTDOc) was reported for comparison.[14] Here, a new member of the bisperylene family is studied for the first time. Two diimide perylenes are joined by the imide groups with no substituent chain in between. The Pr_2 molecule is shown in Fig. 1.

Experimental

Synthesis of *N′,N‴*-dipropyl-*N,N″*-bi[perylene-3,4:9,10-bis(dicarboximide)] (Pr_2)

To a suspension of 4.76 g (0,011 mole) of perylene-3,4,9,10-tetracarboxylic acid monoanhydride mono(*n*-propyl) imide[15,16] in 200 ml of 1-methylpyrrolidin-2-one, stirred under an argon atmosphere, was added 0.16 g (157 μl, 0.0050 mole) of anhydrous hydrazine. The mixture was stirred at room temperature for 30 min then was heated to reflux (202 °C). After 4.5 h the reaction mixture was cooled with stirring to 160 °C then was filtered through a 11 cm glass-fiber filter (Whatman 934AH) in a preheated porcelain funnel. The solid was washed on the funnel with 5 × 100 ml portions of boiling dimethylformamide. The initial filtrate was a dark brown

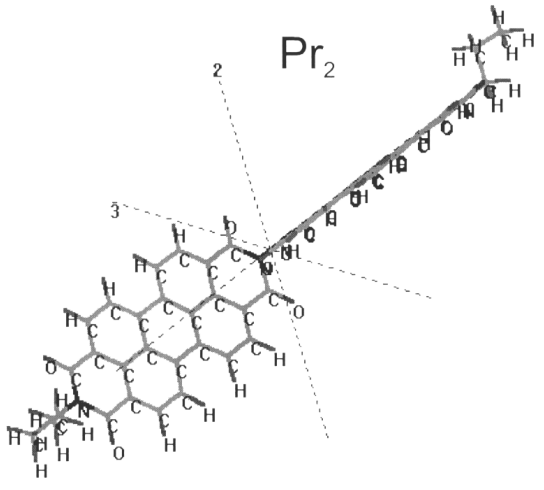

Fig. 1 Chemical structure of the bi(propylperylenediimide) (Pr_2) in the optimum geometry as calculated with AM1 semiempirical quantum calculations.

color. The final hot wash was light orange. The solid was washed with 4×25 ml portions of methanol then was dried at 60 °C to give 3.2 g (74%) of fine grey-black solid, mp 428 °C (decomp.) (by DSC); ^{1}H NMR (300 MHz, ppm, 3:1 $CDCl_3$–trifluoroacetic acid-d, internal TMS): 1.03 (t, 3H, CH_3), 1.84 (m, 2H, CH_2), 4.25 (t, 2H, N-CH_2), 8.89 (m, 8H, aryl-H). Anal. calcd. for $C_{54}H_{30}N_4O_8$: C 75.17, H 3.51, N 6.50; found: C 73.60, H 3.50, N 6.42.

Thin film preparation

The ability of bisperylene materials to form thin films by thermal evaporation without decomposition has been demonstrated in previous work.[13,14] Pr_2 films of different thickness were deposited onto a variety of substrates: transparent and pre-cleaned borosilicate slides (Baxter Cat. M6145) for visible absorption and fluorescence work (they were cleaned by rubbing with absolute ethanol, and subsequent drying under a continuous flow of dry nitrogen gas), polished KBr discs for transmission FTIR and 100 nm mass thickness of silver on glass for reflection absorption infrared spectroscopy. Silver islands of 6 nm mass thickness were used as substrate for SERRS experiments.

Metal deposition was performed in a Balzers vacuum system evaporator, equipped with an Edwards E2M2 rotary vacuum pump which functions as precursor to the Edwards diffusion pump. Silver shots (Aldrich 20,436-6) were thermally evaporated from a cupped tungsten boat, using a Balzers BSV 080 glow discharge/evaporation unit. The background pressure was nominally 10^{-6} Torr, as measured by the Balzers IKR 020 cold cathode gauge. On a substrate preheated to 200 °C, silver was deposited at a rate of 0.05 nm s^{-1} to a total mass thickness of 100 nm. This deposition rate was allowed to stabilize before the shutter was opened. Film thickness and deposition rates were monitored using a XTC Inficon quartz crystal oscillator. The bulk density of silver employed was 10.5 g cm^{-3}, the tooling factor 105%, and the Z-ratio 0.529.

The organic dye was deposited onto the different substrates in a different evaporation system with the same setup aforementioned, with the exception that the substrate was not heated. The perylene pigment was evaporated from tantalum boats and the deposition rate for Pr_2 was about 0.2 nm s^{-1}. The bulk density employed for the Pr_2 material was 1 g cm^{-3}, the tooling factor 92%, and the Z-ratio 0.1. The solutions of the dye were prepared using chloroform (spectroscopic grade, Aldrich) as solvent.

The fluorescence and Raman spectra were recorded using the 514.5 nm line of the Ar^+ laser as an excitation source and both a THR 1000 spectrograph with a liquid nitrogen cooled CCD detector and the Ramanor U1000 double monochromator spectrometer. All spectra were recorded in a back-scattering geometry using a microscope attachment and a $\times 100$ objective. SERRS spectra were also recorded using the 633 nm He–Ne laser line in the Renishaw system 2000. The infrared spectra were recorded with 1 cm^{-1} resolution using a Bomem DA3 FTIR equipped with a liquid nitrogen cooled MCT detector. The FT-Raman spectra were measured on a Bomem Ramspec 150 spectrophotometer with an Nd : YAG laser emitting at 1064.1 nm and equipped with a InGaAs detector. The Raman spectra were recorded with a spectral resolution of 4 cm^{-1}. Semi-empirical quantum chemical calculations, for geometry and frequency optimization, were carried out using AM1 basis sets on Gaussian 94 and HyperChem 5.0.

Results and discussion

Electronic spectra

The absorption spectra of PTC derivatives have been recently calculated and assigned[17,18] The observed visible absorption spectrum consists of one electronic transition with the corresponding vibronic structure. The absorption and emission spectra of Pr_2 solutions in chloroform are shown in Fig. 2. The absorption spectrum shows the characteristic vibronic structure associated with the π–π^* transition of the perylene moiety, with a 0–0 band at 526 nm followed by band maxima at 490 nm, 457 nm and 436 nm. A concentration dependent broad band appears at around 642 nm, probably due to aggregation in solution. The extinction coefficients obtained from the absorbance *vs.* concentration measurements in solution are shown in Table 1.

The fluorescence spectra of the same solutions yielded a mirror image of the absorption spectrum with maxima at 540 nm, 582 nm and a weak band at *ca.* 635 nm.

The absorption and emission spectra of a 120 nm evaporated film of Pr_2 on glass are similar to those of the KBr dispersed pellet and are also shown in Fig. 2. The absorption spectrum of the solid film shows band broadening with maxima close to the monomer absorption at 509 nm and a red shifted maximum at 557 nm. The emission obtained with 514.5 nm excitation is typical of an excimer emitter with a maximum at 688 nm and the same results are obtained for a KBr diluted pellet of Pr_2 with a maximum at 697 nm. It is now known that for thin solid films thicker than 2 monolayers the predominant emission is that of excimers.[11] The molecular stacking and orientational distribution have a significant effect on the spectral profile (bandwidth and symmetry) that explain the differences between the thin solid film and pellet spectra.

Complementary information on the electronic spectra were obtained through computations carried out using the AM1 semi-empirical Hamiltonian as implemented in HyperChem 5, with 7 occupied and 7 unoccupied orbitals used in the configuration interaction. The geometry of the molecule was first fully optimized using AM1 in Gaussian 94, with a convergence limit of 0.01 kcal mol^{-1}. The outcome was a C_1 symmetry molecule with the two macrocycles perpendicular to each other (see Fig. 1) and parameters (distances and derivatives) close to standard values. All frontier orbitals for the Pr_2 molecule are π type. The HOMO is ϕ_{157}, with $\varepsilon_{HOMO} = -8.88$ eV, whereas the LUMO is ϕ_{158}, with $\varepsilon_{LUMO} = -2.51$ eV, which gives a band gap of 6.37 eV, similar to that calculated for monoperylene derivatives.[17,18] In conclusion, the energy mini-

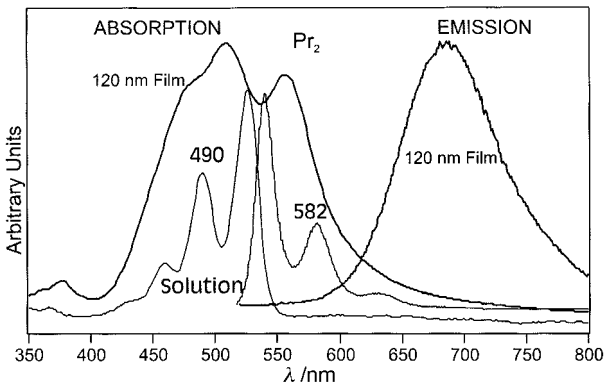

Fig. 2 Absorption and emission spectra of Pr_2 solutions in $CHCl_3$ and of a Pr_2 120 nm evaporated film on glass. The excitation wavelength of the fluorescence spectrum is the Ar^+ laser line at 514.5 nm. The *y*-axis has arbitrary units.

Table 1

Band center/nm	Coefficient/dm^3 mol^{-1} cm^{-1}
436	1.11×10^3
457	2.69×10^3
490	1.17×10^4
526	1.63×10^4

mization gives a non planar system with the two planar PTC moieties perpendicular to each other. At the same time, the emission spectra clearly indicate that excimer formation takes place producing a broad band fluorescence (Fig. 2). The question remains about the long range organization in thin solid films of the material.

Vibrational spectra

The vibrational spectra of the Pr_2 material is presented in Fig. 3. The *y*-axis is in arbitrary units to allow Raman and infrared spectra in one graph. The reference spectrum for the assignment of the IR allowed normal modes is that of an isotropic dispersion of Pr_2 in KBr shown in Fig. 3. Since the KBr pellet spectrum represents a random spatial distribution of monomer and aggregates it is also the reference for the molecular organization in thin solid films. For a molecular system with 282 normal modes of vibration, it is reasonable to limit the discussion of normal mode assignment to a few characteristic in-plane and out-of-plane vibrations of the chromophore moiety.[19–21] The computation of fundamental vibrational wavenumbers using the AM1 was successful and all eigenvalues were positive. The most characteristic in-plane molecular vibrations of the PTC group of the Pr_2 molecule are the carbonyl stretching modes: the antisymmetric stretching at 1656 cm^{-1} and the symmetric C=O stretching at 1694 cm^{-1}. The symmetric mode is also observed in the FT-Raman spectrum at 1694 cm^{-1}. The dynamic dipoles of the symmetric and antisymmetric carbonyl stretches are in the PTC plane and they are perpendicular to each other, which makes them excellent probes for orientational studies.[22] The calculated infrared intensities predicted three (accidentally degenerate) strong C=O fundamentals, and in fact three C=O bands can be identified in the IR spectrum and listed in Table 2. The strongest in-plane perylene C=C stretching vibration is observed at 1594 cm^{-1} as seen in Fig. 3. A weak band at 1579 cm^{-1} is also a C=C stretch of the perylene ring. Both of these modes are clearly seen in the FT-Raman spectrum with their relative intensity reversed (see Fig. 3). The computed spectrum predicts three strong IR bands in this region at 1590, 1558 and 1450 cm^{-1}. The out-of-plane wagging vibrations of the perylene ring have a dynamic dipole perpendicular to the perylene plane and thereby perpendicular to components of the dipole moment derivatives of the carbonyl or C=C stretching vibrations. The out-of-plane modes are observed with characteristic wavenumber and relative intensity at 738 cm^{-1} and 810 cm^{-1}, and they are assigned to the C–H wagging vibrations. The calculated IR spectrum predicts two strong (accidentally degenerate) bands in this region at 753 and 853 cm^{-1} in good agreement with the observations. The assignment of the in-plane and out-of-plane modes of the perylene moiety provides the basis for the discussion of the average molecular orientation of the chromophores in the evaporated film. The assignment of characteristic infrared bands is presented in Table 2, while Table 3 compiles observed Raman wavenumbers, relative intensities and bandwidths for the Pr_2 molecule. Notably, the middle infrared and FT-Raman spectra of Pr_2 are relatively simple. The large number of modes are seen in the far-infrared region, which is a consequence of very similar infrared cross sections for these highly coupled deformation vibrations. The observed far-IR wavenumbers are: 86, 137, 187, 219, 388, 436, 466, 494, 515, 540, 575, 591 and 605 cm^{-1}. The latter three wavenumbers are also seen in the middle infrared spectrum with very weak relative intensity. The 219 cm^{-1} and the 540 cm^{-1} wavenumbers are observed in the resonance Raman spectrum.

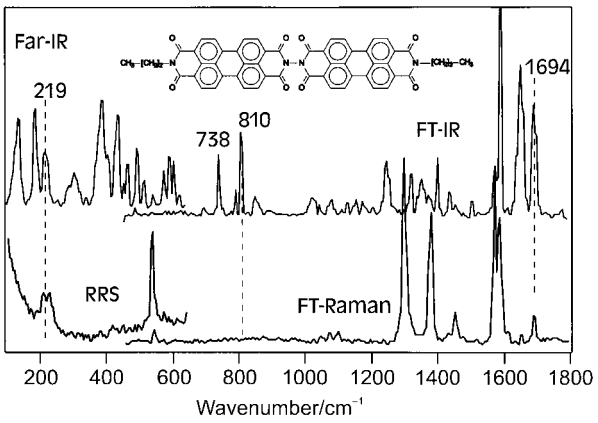

Fig. 3 Vibrational spectra of Pr_2. FT-Raman of the solid and low wavenumber region of the RRS spectrum of Pr_2. FTIR spectrum of Pr_2 dispersed in a KBr pellet and far-IR spectrum in polyethylene windows. The *y*-axis has arbitrary units.

The off resonance FT-Raman spectrum of the bulk in a pellet and the low region of Resonance Raman Scattering (RRS) of a 120 nm evaporated film are presented in Fig. 3. Insignificant differences are observed between the two spectra. Both the resonant and the non-resonant spectra are completely determined by the vibrational modes of the perylene chromophore. The characteristic vibrational modes of the perylene moiety are observed in the FT-Raman at 1300 cm^{-1}, 1379 cm^{-1}, 1574 cm^{-1} and 1590 cm^{-1}. However, only the FT-Raman spectrum shows the symmetric carbonyl stretching band at 1694 cm^{-1}. The variation in the bandwidth of Raman bands may be explained by band overlapping due to the fact that the two PTC moieties that form the Pr_2 compound have vibrational modes that are accidentally degenerate in wavenumber.

Infrared spectra and molecular organization

Vibrational spectroscopy provides several observables that may be used to extract physical information from thin solid films: the resonance band position, the band shape, and the band intensity. It is this wealth of information that makes vibrational spectroscopy a unique optical probe for determination of the overall structure, chemical, mechanical and localized intermolecular interactions in thick and submicron thin solid films. In particular, the intensity in the vibrational spectrum of thin solid films can be explained in terms of the polarization of the incoming infrared beam and the directionality of the dipole moment derivatives. For instance, the selection rules operating in the specular reflection absorption infrared spectroscopy (RAIRS) have been extensively used to determine the orientation of nanometric organic films thermally deposited on a reflecting metal surface.[23] Transmission and reflection spectroscopic techniques can be used concurrently to enable a definitive account of the molecular orientation of perylene molecules.[22]

The molecular orientation on a film creates a film anisotropy that can be extracted using the change in relative intensity observed in the film's spectra recorded in the transmission geometry. In Fig. 4, the transmission IR spectrum of a 100 nm Pr_2 film deposited onto KBr is compared with the reflection-absorption IR spectrum of a 100 nm Pr_2 film deposited onto a smooth silver film (100 nm). In the transmission geometry, the polarization of the incident radiation always lies along the substrate surface (shown in Fig. 4). For the vacuum evaporated film, with a particular molecular orientation in the direction perpendicular to the substrate, only bands with a change in dipole moment parallel to the substrate surface will be intense. Infrared bands corresponding to a change in dipole moment perpendicular to the substrate surface will not absorb. In the RAIRS case, the reflecting surface polarizes the light perpendicular to the surface plane. Therefore, the intensity of

Table 2 Observed IR wavenumbers (cm^{-1}), relative intensities (in parentheses) and full width at half maximum (FWHM) in cm^{-1} for Pr_2

Pellet		Film		RAIRS		
cm^{-1}	FWHM	cm^{-1}	FWHM	cm^{-1}	FWHM	Assignment
487 (3)	6					Ring deformations
580, 592, 605		656 (16)	9			Ring deformations
738 (33)	8	742 (5)	8	739 (32)	9	C–H per. wag
754 (4)	12	753 (2)	10	752 (12)		C–H per. wag
794 (13)	5	795 (11)	5	795 (7)	6	alkyl bending
810 (41)	5	811 (13)	5	811 (37)	5	C–H per. wag
851 (7)	5	852 (4)	13	851 (6)	9	C–H per. wag
856 (8)	5					
966 (2)	17	950 (2)	7	952 (2)		C–H bending
1025 (19)	20	1023 (1)	15			C–H bending
1047 (6)	10	1044 (1)	17			C–H bending
1082 (17)	20	1084 (6)	12	1084 (1)		C–H bending
1173 (5)	14	1184 (6)	13	1183 (1)		C–H bending
1249 (30)	19	1243 (7)	13	1248 (10)	14	Alkyl bending
1270 (4)	17	1271 (33)	20	1272 (4)	14	Alkyl bending
1287 (3)	8			1280 (5)	15	Alkyl bending
1324 (22)	11			1323 (10)	15	Alkyl bending
1351 (16)	12	1345 (45)	18	1346 (19)	14	C–N stretch
1359 (18)	10	1358 (19)	8	1357 (31)	17	C–N stretch
1375 (7)	13	1369 (9)	13	1375 (10)	17	C–N stretch
1404 (31)	7	1402 (21)	6	1404 (23)	7	Ring stretch
1438 (13)	11	1437 (14)	13	1438 (16)	20	CH_2 scissors
1579 (24)	17	1578 (32)	15	1580 (10)		C=C Ring stretch
1594 (100)	8	1594 (82)	9	1596 (83)	8	C=C Ring stretch
1644 (19)	17			1643 (12)		C=O stretch
1656 (77)	17	1656 (33)	16	1660 (71)	19	C=O stretch
1694 (64)	18	1694 (100)	21	1696 (100)	20	C=O stretch

Table 3 Observed Raman wavenumbers (cm^{-1}), relative intensities (in parentheses) and full width at half maximum (FWHM) in cm^{-1} for Pr_2

FT-Raman		RRS 514.5 nm		SERRS 514.5 nm		SERRS 633 nm		
cm^{-1}	FWHM	cm^{-1}	FWHM	cm^{-1}	FWHM	cm^{-1}	FWHM	Assignment
544 (7)	9	542 (20)	11	551 (18)	19	551 (3)	20	Per. deformation
						562 (25)	11	
573 (1)		576 (3)	8					Alkyl deformation
1049 (3)	13					1064 (13)	13	C–H bend
1074 (4)	12	1074 (6)		1075 (6)	16	1076 (3)	20	C–H bend
1098 (5)	11							C–H bend
1300 (100)	12	1300 (86)	17	1295 (84)	19	1294 (100)	24	C–H bend + ring str.
1319 (7)	24	1312 (18)	32	1308 (20)				CH_2 bend
1379 (71)	13	1377 (100)	24	1376 (100)	20	1382 (65)	19	Per. ring str.
1455 (17)	10	1454 (10)	11	1452 (16)	20	1452 (12)	16	Per ring str.
1574 (98)	9	1571 (77)	11	1571 (31)	6	1574 (84)	18	C=C stretch
1590 (65)	14	1587 (57)	21	1598 (10)	30	1601 (6)	30	C=C stretch
1612 (6)	16	1610 (10)	21					C=C stretch
1694 (16)	10			1696 (4)	23			C=O stretch

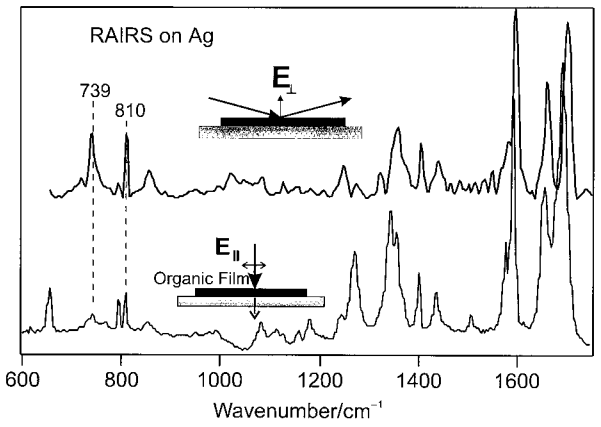

Fig. 4 Infrared transmission and reflection–absorption spectra of a 100 nm Pr_2 film deposited onto a KBr disc and a 100 nm Ag smooth film, respectively.

vibrational modes with a dynamic dipole perpendicular to the surface are enhanced and those modes parallel to the surface are suppressed.[23] No substantial differences were observed in the relative intensities of the out-of plane modes observed in the RAIRS spectrum and the spectrum of the KBr reference (Fig. 3 and 4), allowing us to conclude that there is no preferential face-on long range organization in the direction perpendicular to the plane of the substrate. There is, however an increase in the relative intensity of the symmetric C=O stretching band (1696 cm^{-1}) with a dipole moment derivative component along the long molecular axis. The latter may be interpreted as a slight tilted (head-on) long range organization in the film. The thin solid film evaporated onto the KBr surface (lower trace in Fig. 4) produced a spectrum that represents a minor deviation from the reference. It can be seen that the out-of-plane modes at 739 cm^{-1} and 810 cm^{-1} are observed with a decreased relative intensity when compared with the symmetric C=O stretch (1694) in the transmission spectrum. The latter may be interpreted as indication of some face-on molecular orientation, a different alignment from what

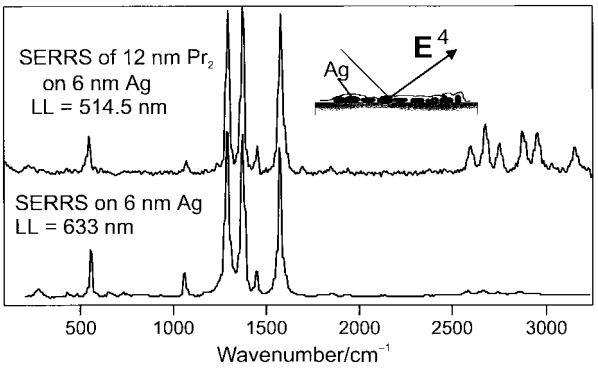

Fig. 5 Surface enhanced resonant Raman spectrum of a 12 nm Pr_2 film on 6 nm Ag film with a plasmon absorption at 510 nm. Upper trace is the SERRS spectrum with 514.5 nm excitation wavelength and the lower trace is the SERRS spectrum with He–Ne 633 nm excitation wavelength. The *y*-axis units are arbitrary.

was extracted from the film on smooth metal surface. However, the degree of this long range organization is far less than what was observed for 1,8-bis(3-chlorobenzylimidoperylenyl)octane (BPTDOc) where an octyl group is placed between the two PTC moieties. The lack of a strong molecular alignment in Pr_2 can only be explained by the findings of the geometry optimization indicating that the two planar PTC groups are perpendicular to each other. Such molecular geometry seems also to be predominant in the solid state.

Surface-enhanced resonant Raman scattering

In Fig. 5, the surface-enhanced resonance Raman scattering (SERRS) spectra of a 12 nm film of Pr_2 deposited onto a 6 nm silver island film and excited with both the Ar^+ 514.5 nm and the He–Ne 633 nm laser lines, are shown. The SERRS spectra are simply the amplified version of the RRS spectrum. Both spectra are entirely due to the PTC moiety. Notably, the carbonyl stretches seen in the FT-Raman are not observed in the RRS or SERRS spectra of Pr_2. The SERRS spectra as well as the FT-Raman spectrum are very simple for such a large molecular system and contain less than 10 characteristic fundamentals. One important difference between the SERRS spectra excited at 514.5 nm and 633 nm is the relative intensity of the combinations and overtones. From Fig. 2, it can be seen that the 514.5 nm laser line is in full resonance with the absorption spectrum of the nanometric film and it contains combinations and overtones with a strong relative intensity. The spectrum obtained with the 633 nm excitation is a pre-resonance Raman spectrum, and a low relative intensity of overtones and combination bands is consistent with it. Appreciable relative intensity of combinations and overtones is only achieved in the RRS spectrum and they are not observed in the FT-Raman spectrum. The relative intensity differences between the Red-SERRS (He–Ne excitation) and the Green-SERRS (Ar^+ excitation) are minimal (with the exception of the combinations and overtones) and the observed wavenumbers are the same in RRS and SERRS. It is then concluded that the Pr_2 is physically adsorbed on the silver islands, a fact of considerable importance for its possible practical analytical applications. It is also evident from the two spectra shown in Fig. 5 that the bands observed in the 2900–3100 cm^{-1} region correspond to overtones and combinations, while the C–H stretching vibrations are not seen in the spectrum. In summary, the spontaneous Raman scattering (FT-Raman), the RRS and the SERRS spectra of the Pr_2 molecule are not very different from those of the monoperylene tetracarboxylic derivatives.

Conclusion

The member of a new class of perylene derivatives (bisperylenes), *N′,N‴*-dipropyl-*N,N″*-bi[perylene-3,4:9,10-bis(dicarboximide)] has been characterised by optical spectroscopy. It has been demonstrated that thin solid films of this material can be easily fabricated by vacuum thermal evaporation. The energy minimization gives a non planar system with the two planar PTC moieties perpendicular to each other. The molecular structure with perpendicular planes does not favor molecular stacking and correspondingly the infrared spectra of films show evidence of marginal molecular organization in the perpendicular direction of thin solid films formed on silver or KBr. This behavior is in contrast with the common tendency to stacking and molecular alignment observed in perylene tetracarboxylic derivatives. However, the formation of excimers in solid films was clearly established by the presence of the characteristic broad band in the fluorescence spectrum.

NSERC of Canada is gratefully acknowledged for financial support.

References

1 P. E. Burrows, Y. Zhang, E. I. Haskal and S. R. Forrest, *Appl. Phys. Lett.*, 1992, **61**, 2417.
2 A. L. Moser, *Phthalocyanine Research and Applications*, CRC Press, Boca Raton, 1990.
3 *Phthalocyanines Properties and Applications*, ed. C. C. Leznoff and A. B. P. Lever, VCH Publishers, Inc., New York, 1989.
4 C. Taliani and L. M. Blinov, *Adv. Mater.*, 1996, **8**, 353.
5 C. A. Jennings, R. Aroca, G. J. Kovacs and C. Hsaio, *J. Raman Spectrosc.*, 1996, **27**, 867.
6 A. Hoshino, S. Isoda, H. Kurata and T. Kobayashi, *J. Appl. Phys.*, 1994, **76**, 4113.
7 C. Ludwig, B. Gompf, W. Glatz, J. Petersen, W. Eisenmenger, M. Mobus, U. Zimmermann and N. Karl, *Z. Phys. B*, 1992, **86**, 397.
8 C. Ludwig, B. Gompf, W. Glatz, J. Petersen and W. Eisenmenger, *Z. Phys. B*, 1994, **93**, 365.
9 T. Schmitz-Hubsch, T. Fritz, F. Sellam, R. Staub and K.Leo, *Phys. Rev. B*, 1997, **55**, 7972.
10 C. M. Fisher, M. Burghard, S. Roth and K. v. Klitzing, *Europhys. Lett.*, 1994, **28**, 129.
11 D. Schlettwein, A. Back, B. Scilling, T. Fritz and N. R. Armstrong, *Chem. Mater.*, 1998, **10**, 601.
12 D. Lamoen, P. Ballone and M. Piranello, *Phys. Rev. B*, 1966, **54**, 5097.
13 S. Rodriguez-Llorente, R. Aroca, J. Duff and J. A. DeSaja, *Thin Solid Films*, 1998, **317**, 6037.
14 S. Rodríguez-Llorente, R. Aroca and J . Duff, *J. Mater. Chem.*, 1998, **8**, 629.
15 H. Troster, *Dyes Pigments*, 1983, **4**, 171.
16 E. Spietscha and H. Troster, US Patent 4 709 129 (November, 1987).
17 R. Mercadante, M. Trsic, J. Duff and R. Aroca, *J. Mol. Struct. (Theochem)*, 1997, **394**, 215.
18 M. Adachi, Y. Murata and S. Nakamura, *J. Phys. Chem.*, 1995, **99**, 14 240.
19 R. Aroca, A. K. Maiti and Y. Nagao, *J. Raman Spectrosc.*, 1993, **24**, 227.
20 A. K. Maiti, R. Aroca and Y. Nagao, *J. Raman Spectrosc.*, 1993, **24**, 351.
21 R. Aroca and R. E. Clavijo, *Spectrochim. Acta*, 1991, **47A**, 271.
22 E. Johnson and R. Aroca, *Appl. Spectrosc.*, 1995, **49**, 472.
23 M. K. Debe, *Prog. Surf. Sci.*, 1987, **24**, 1-282.

Paper 8/03180K